

A ‘Bottom-up’ Redefinition for Mobility and the Effect of Poor Tube-Tube Contact on the Performance of CNT Nanobundle Thin Film Transistors

Ninad Pimparkar* and Muhammad Ashraful Alam

School of Electrical and Computer Engineering, Purdue University, West Lafayette, IN 47907-1285, USA.

*Phone: (765) 409 3109 Fax: (765) 494 2706 Email: ninad@purdue.edu

Background: There have been many recent reports on Nanobundle Thin Film Transistors (NB-TFTs) based on percolating network of randomly-oriented Silicon nanowires (NW) and Carbon nanotubes (NT) or sticks in general (Fig. 1) with hopes of approaching mobility (μ) of *single* CNT/NW transistors (μ_i), without being limited by placement issues and low on current, I_{ON} . High- μ and highly homogenous NB-TFTs have potential to replace currently-dominant materials like amorphous (a-)Si or poly (p-) Si in applications in macroelectronics such as displays, e-paper, bio-chemical sensors, conformal radar, solar cells and others¹⁻⁴. Puzzling, however, is the fact that the reported values of μ of NB-TFT (μ_{NB}) – calculated by traditional ‘top-down’ effective media approach (EMA) -- is not only far poorer than single CNT transistors, but also appears to be a random function of experimental conditions^{2,3,7,8}. In this paper, we show that (a) the randomness of μ_{NB} is not intrinsic, but rather signals the breakdown of ‘top-down’ definition μ_{NB} and a percolation-theory based ‘bottom-up’ definition of μ_{NB} can consistently interpret the results, and (b) the difference between μ_i and μ_{NB} can be attributed to geometrical parameters of transistor (!) such as tube density (D), tube length (L_S), channel length (L_C), etc. and tube-tube contact (C_{ij}). Our results not only provide specific guidance to achieve geometry-specific theoretical limits of μ_{NB} , but also suggest simple characterization of technology-critical C_{ij} from a few simple measurements.

Stick Percolation Model: We constructed a sophisticated first-principle numerical stick-percolation model for the above NB-TFTs by generalizing the random-network theory. The model¹ randomly populates a 2D grid by sticks of fixed length (L_S) and random orientation (θ) (Fig. 1) and determines I_{ON} through the network by solving the percolating electron transport through individual sticks. In contrast to classical percolation, the NB-TFT is a heterogeneous network: 1/3 of the CNTs are metallic and remaining 2/3 are semiconducting. Since, L_C and L_S are much larger than the phonon mean free path, linear-response transport (small V_{sd} and constant V_g obviates the need to solve the Poisson equation explicitly) within individual stick segments of this random stick-network system is well described by drift-diffusion theory¹. The low bias drift-diffusion equation, $J = q\mu n d\phi/ds$, when combined with current continuity equation, $dJ/ds = 0$, gives the non-dimensional potential ϕ_i along tube i as $d^2\phi_i/ds^2 - C_{ij}(\phi_i - \phi_j) = 0$. Here, s is the length along the tube and $C_{ij} = G_0/G_1$ is the dimensionless charge-transfer coefficient between tubes i and j at their intersection point, and G_0 ($\sim 0.1 e^2/h$)⁵ and $G_1 (= qn\mu/\Delta x)$ ¹ are mutual- and self-conductance of the tubes, respectively. Here, n is carrier density, μ is mobility and Δx is grid spacing. The stick percolation networks are non-classical 2D conductor and satisfy the finite size scaling relationship⁶ $I_{ON} \sim k\zeta(L_C, L_S) = k/L_S(L_S/L_C)^m$ (Fig. 2d). Here, k is material specific constant and the exponent $m(DL_S^2)$ is universal constant that depends *only* on the areal tube density (D) and L_S (Fig. 2d). We now use this model to resolve the two puzzles of μ_{NB} discussed above:

(a) Puzzle of Randomness of Long-Channel μ_{NB} : In the literature, researchers universally use the ‘top-down’ definition of $\mu = (dI_D/dV_G/V_D)L_C/(L_W C_{OX})$ to characterize NB-TFTs (Fig. 3b). This μ is geometry-dependent and appears to reduce with lower density and longer L_C (Fig. 3b, blue squares)! Actually, μ for a percolative network should not be defined in this manner at all and a proper ‘bottom-up’ definition, $\mu_{NB} \sim (dI_D/dV_G/V_D) L_S/(L_C/L_S)^m / (L_W C_{OX})$, provides a device geometry independent value and allows a *comparison* between the mobilities from different labs^{2,7,8} as shown in Fig. 3b and c. Not surprisingly, for high density networks (Fig. 3, red circles) with, $m \sim 1$, both the definitions give same result i. e. $\mu \sim \mu_{NB}$.

(b) Short and Long Channel Transistors and the role of C_{ij} : The second puzzle is that experiments often show that the μ_{NB} of the long channel ($L_C > L_S$) NB-TFT is almost an order of magnitude smaller than that of a short channel ($L_C < L_S$) device where the tubes bridge the source and drain directly^{2,4,9}. Hence, we need to reanalyze the role of imperfect C_{ij} to explore differences between short and long- L_C transistors. Fig. 4 a, b and c show the simulated I_{ON} vs. L_C for short and long channel NB-TFTs for high and low values of C_{ij} . Note the increasingly abrupt reduction in I_{ON} at $L_C/L_S \sim 1$ with reduction in C_{ij} (Fig. 4a through c). The plot of the abrupt drop in current (R_{ij}) at the transition point as a function of C_{ij} for different tube-density, D in Fig. 4e shows that $R_{ij} \propto C_{ij}$ for low values of C_{ij} or poor tube-tube contact (Fig. 4b and c) but saturates to 1 for higher C_{ij} (Fig. 4a), or for good tube-tube contact, as expected. Finally, Fig. 4d plots the exponent m (see Fig. 2), for different densities are a function of C_{ij} . m increases monotonically with decreasing C_{ij} as the contribution of tube-tube resistance to the total device resistance goes up. The ratio of mobilities (μ_{NB}) for short ($L_C > L_S$) and long ($L_C < L_S$) channel NB-TFTs can be directly related to C_{ij} using Fig. 4e, resolving the puzzle discussed above. Moreover, once D is determined from SEM images and m from Fig. 2, C_{ij} can also be read out from Fig. 4d providing an experimental measure of a technology-critical parameter for design of NB-TFTs.

Conclusion: We have redefined the mobility for NB-TFTs from the ‘bottom-up’ perspective using the stick percolation model to allow direct comparison of NB-TFT mobilities across different labs^{2,7,8} and with other competing technologies such as a-Si and p-Si. We have also suggested a simple experimental measure of the critical tube-tube contact parameter to allow design of optimized transistors.

References: [1] S. Kumar, et al., Phys. Rev. Lett. 95 (2005). [2] E. S. Snow, et al., Appl. Phys. Lett. 82, 2145 (2003). [3] L. Hu, et al., Nano Lett. 4, 2513 (2004). [4] S. J. Kang, et al., Nature Nano. (In Press). [5] M. S. Fuhrer, et al., Sci. 288, 494 (2000). [6] D. Stauffer, et al., *Intro. to percolation Theory* (1992). [7] C. Kocabas, et al., Nano Lett. (In Press). [8] S. H. Hur, et al., J. of the Ame. Chem. Soc. 127, 13808 (2005). [9] E. Artukovic, et al., Nano Lett. 5, 757 (2005).

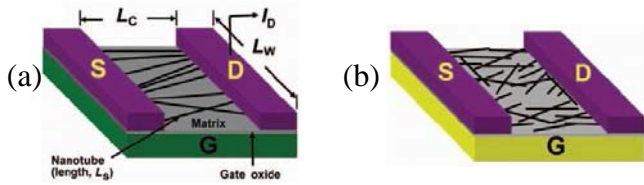


Fig. 1: Schematic diagrams for NB-TFT with (a) short channels ($L_C < L_S$, nanosticks directly bridge source S and drain D) and (b) long channels ($L_C > L_S$, electrons must percolate through the nanostick network to contribute to the drain current). L_C is channel length, L_W is channel width, L_S is stick length; S, D and G are source, drain, and gate electrodes, respectively.

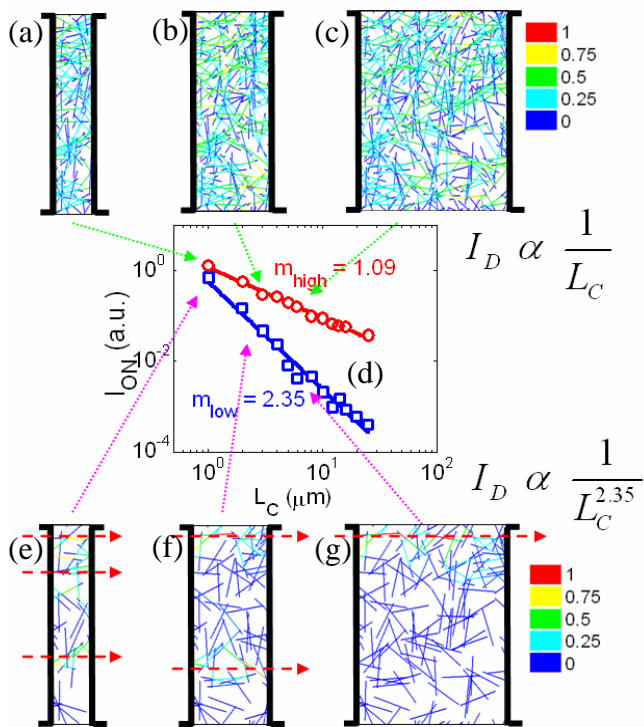


Fig. 2: Normalized current distribution for network with high (a, b, c) and low (e, f, g) density for $L_C/L_S = 1, 2, 4$, respectively. (d) I_{ON} vs. L_C plot for various tube densities (D). The symbols show experimental data from Ref. [3] and the lines show the simulations using the stick percolation model. The arrows indicate the density and L_C to which each of the samples represent. The equations show the current dependence on L_C with appropriate current exponent, m . A common color bar for all the figures is also shown. The dashed arrows in (e, f, g) show the current paths.

Acknowledgements: The authors would like to express their sincere gratitude towards S. Kang, C. Kocabas, and Prof. J. A. Rogers for helpful discussions. This work was supported by the Network of Computational Nanotechnology and the Lilly Foundation.

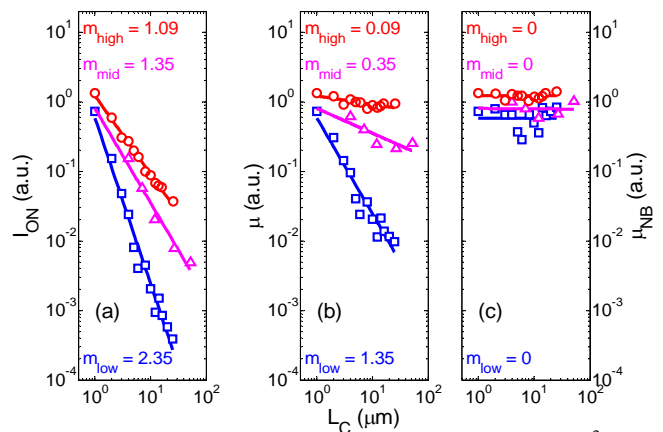


Fig. 3: (a) Experimental I_{ON} vs. L_C plot for high³ (red), medium⁴ (magenta) and low³ (blue) density random network. The current exponent given by the slope of the lines are given by $m = 1.09, 1.35$, and 2.35 , respectively. (b) Mobility (μ) vs. L_C plot for same networks using the conventional definition of mobility. The mobility is dependent on channel length with exponents, $m = 0.09, 0.35$, and 1.35 , respectively. (c) The NB-TFT mobility from the ‘Bottom-up’ perspective vs. L_C . Note that this mobility is independent of L_C .

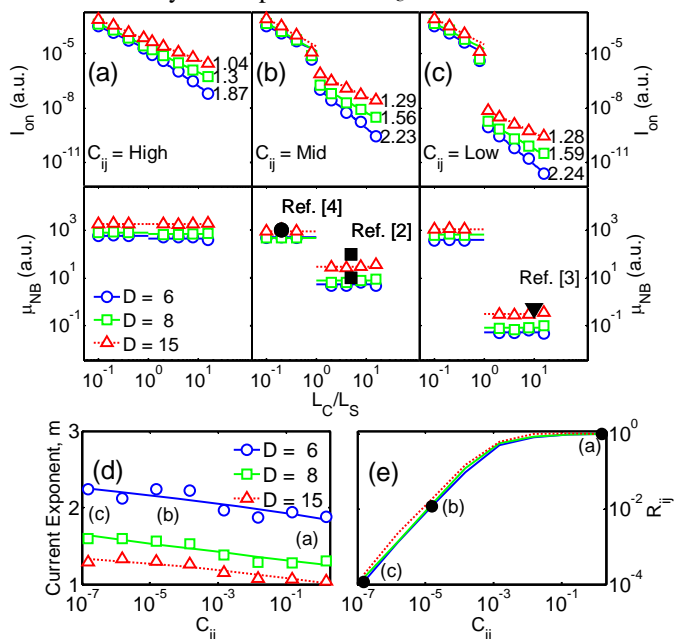


Fig. 4: Simulated I_{ON} vs. L_C/L_S plot (a) high (b) medium and (c) low tube-tube contact parameter, C_{ij} . The lower panel shows the corresponding mobilities (μ_{NB}). The black symbols in the lower panels of a, b and c map the reported mobility values from various labs as indicated by the reference numbers. Here we have assumed that all the tubes are same length (L_S) for different density (D) random tube networks. Note the abrupt transition in (b, c) at $L_C/L_S = 1$ which is a result of bad tube-tube contact. Also note that the current exponents, m , for $L_C > L_S$ change with C_{ij} . (d) Current exponent, m vs. C_{ij} for different density tube network. The exponents are relatively insensitive to the tube-tube contact, however (e) shows the normalized drop in current (R_{ij}) at the transition point $L_C/L_S = 1$. R_{ij} is insensitive to the tube density (D). The dark circles show corresponding to the figures a, b, c as indicated